Benchmarking of lamina failure tests from WWFE-I and WWFE-II with a three parameter micromechanics based matrix failure theory

Kedar A. Malusare*, Ray S. Fertig III**
*Graduate Student, Mechanical Engineering, University of Wyoming,
kmalusar@uwyo.edu
**Assistant Professor, Mechanical Engineering, University of Wyoming,
rfertig@uwyo.edu

Abstract

The use of fiber reinforced composites in the wind energy industry is growing rapidly. Owing to their increasing importance, it is critical to develop tools to accurately predict their complex behavior under different loading conditions. However, their heterogeneous microstructure and inherent anisotropy make failure prediction very difficult. Two well-known composite failure benchmarks, World-Wide Failure Exercise I (WWFE-I) and World-Wide Failure Exercise II (WWFE-II) compared leading failure theories from around the world with one another and with actual test results. This paper presents a three-parameter micromechanics-based composite failure theory which uses constituent-level stresses to predict matrix-dominated composite failure. A representative volume element (RVE) of the microstructure is used to extract constituent stresses for use with the failure theory. The merit of the failure theory lies in its simplistic calibration which requires just three parameters that can be obtained from three standard composite failure tests (transverse tension, transverse compression and in-plane shear). This theory is benchmarked against lamina failure test data from WWFE-I and WWFE-II and compared with the failure theories that performed comparatively well in WWFE-I and WWFE-II. Our results show that for most of the test cases the predictions of the theory were in close agreement with the test data.

Key Words: Composite materials, failure modeling, benchmarking, WWFE-I, WWFE-II

Introduction

Modern composite materials constitute a significant portion of engineered materials market ranging from everyday products to sophisticated niche applications [1]. Unlike conventional homogeneous materials like metals, the properties of composite materials can be tailored to meet the structural demands of the end product, which results in significant weight and cost savings. One of the sectors where fibrous composites are a lucrative choice of materials is the wind energy sector. It is important to increase renewable energy production, particularly wind energy generation, to achieve the goal of reducing our dependency on fossil fuels. This can be realized by installing and expanding many on-shore and off-shore wind farms built with large and extra-large wind turbines. The durability and longevity of a wind turbine can be enhanced if the wind blade materials have high stiffness and strength, and fatigue and environmental resistance. Fibrous composites have been utilized extensively in wind turbines because they offer all the above advantages. Wind turbine blades are exposed to a variety of complex external loads originating from wind, gravity and other natural elements. In order to ensure durability of the turbine blade, reliable failure theories are needed that can predict failure of the blade materials. The approach in this paper is to use multiscale modeling to predict constituent-level failure. The focus of this work will be on benchmarking an existing matrix failure criterion, comparing it with some of the leading failure theories, and suggesting areas for enhancement.

`

Failure Modeling

The Maximum Distortional Energy, or von Mises, criterion is the most widely used criterion for predicting yielding in isotropic metals [2]. Composite materials, unlike metals, are anisotropic making failure prediction a complicated mechanism. For composite materials, failure criteria can be broadly categorized into three groups: limit criteria, interactive criteria, and separate mode criteria [3]. The failure theories falling under limit criteria (e.g. maximum stress) predict failure load by comparing lamina level stresses (σ_{11}, σ_{22} and τ_{12}) with corresponding strengths separately. They do not consider interaction among the different stresses and consequently give the most conservative results. The interactive failure theories (e.g Tsai-Wu [4] and Tsai Hill) predict failure load using a quadratic or higher order polynomial equation which involves all the stress components. The onset of failure is assumed when this equation is satisfied. Separate mode criteria are failure theories that have separate matrix failure criterion and fiber failure criterion. Failure load is predicted by equations which depend on either one or more stress components. Hashin [5], Christensen [6] and Puck [7] failure criterion are some of the examples of separate mode failure criteria. Failure theories may also be classified as meso-mechanical or micro-mechanical depending upon the kind of stresses used to predict failure. Meso-mechanical failure theories use lamina level stresses to predict failure of a lamina, whereas micro-mechanical failure theories employ constituent level stresses to predict failure of a constituent of a lamina. To compare the different failure theories and assess the maturity of different composite failure criteria, Soden, Kaddour and Hinton organized the World Wide Failure Exercises [8] [9]. These composite failure benchmarks contain detailed assessments of different theories and their approaches for predicting the failure response of polymer composite laminates under complex states of stress. The different failure theories were benchmarked against carefully selected test cases after which they were assessed qualitatively. Puck [7], Zinoview [8], Tsai [9] and Bogetti [10] were ranked highest [11] in the first World Wide Failure Exercise (WWFE-I) and Carrere [12], Pinho [13], Cuntze [14] and Puck [15] were ranked highest [16] in the second World Wide Failure Exercise (WWFE-II) for their predictions and descriptions of failure mechanics in composite materials. One major drawback that is evident in all these theories is the use of a substantially large number of input parameters (from 50-75) and thus difficult in calibrating them.

The micromechanical matrix failure theory used in this paper requires three parameters, which all have physical meaning, and utilizes volume-average constituent level stresses to predict failure of a constituent (matrix or fiber here) and thereby of the composite. The merit of the failure theory lies in its simplistic calibration which is required to obtain the three parameters required to predict failure load under any composite state of stress. The matrix failure theory is outlined below [17]

$$B_t\{I_t\}^2 + \frac{1}{1 - \dfrac{\beta}{\tau_0}\{-I_h\}}\left[B_{s1}I_{s1} + B_{s2}I_{s2}\right] = 1 \tag{1}$$

where B_t, B_{s1}, B_{s2} represent the coefficients of the stress invariants;

I_t, I_{s1}, I_{s2}, I_h represent the invariants of matrix stress tensor,

τ_0 represents the shear strength of the matrix,

and β represents pressure strengthening due to compressive loading (~ 0.35) [18].

`

The values of B_i are determined from three composite static failure tests: *transverse tension, transverse compression, and in-plane shear*, all of which involve failure of the matrix constituent. The invariants are computed from the volume average matrix stresses as follows

$$I_t = \frac{\sigma_{22}^m + \sigma_{33}^m + \sqrt{\left(\sigma_{22}^m + \sigma_{33}^m\right)^2 - 4\left(\sigma_{22}^m \sigma_{33}^m + \sigma_{23}^m \sigma_{23}^m\right)}}{2} \tag{2}$$

$$I_{s1} = \sigma_{12}^{m\,2} + \sigma_{13}^{m\,2} \tag{3}$$

$$I_{s2} = \frac{1}{4}\left(\sigma_{22}^m - \sigma_{33}^m\right)^2 + \sigma_{23}^{m\,2} \tag{4}$$

$$I_h = \sigma_{22}^m + \sigma_{33}^m \tag{5}$$

where I_t corresponds to the maximum tensile stress normal to the fiber, I_{s1} is related to the in-plane shear, I_{s2} is related to the transverse shear, and I_h represents the pressure on the maximum transverse shear.

The fiber failure criterion is outlined below

$$\frac{\sigma_{11}^f}{S_{11}^{f+}} = 1 \qquad \text{or} \qquad \frac{\sigma_{11}^f}{S_{11}^{f-}} = 1 \tag{6}$$

where S_{11}^{f+} is the longitudinal tensile strength of the fiber and S_{11}^{f-} compressive strength of the fiber.

The constituent level stresses were extracted from a Representative Volume Element (RVE) of an idealized microstructure of a hexagonally packed fiber reinforced composite, shown in Fig. 1. The RVE has periodic boundary conditions enforced on all its sides and was subjected to six types of loads $\left(\sigma_{11}, \sigma_{22}, \sigma_{33}, \tau_{12}, \tau_{13}, \tau_{23}\right)$, which generated stresses in the fiber and the matrix regions. After extracting stresses from the fiber and the matrix regions, volume average constituent stresses were computed. There exists a mapping X between the composite and constituent stresses, which can be used to compute constituent level stresses for any type of composite load state. This mapping can be computed as shown below [19]
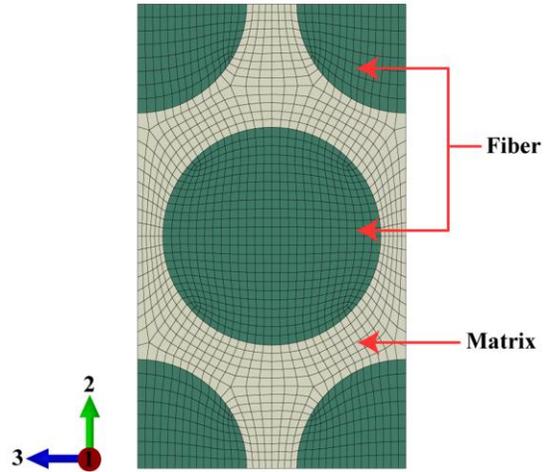
Figure 1 : The RVE with hexagonal fiber packing

$$_L X_i^f = \frac{\sigma_i^f}{\sigma_L^c} \qquad \text{and} \qquad _L X_i^m = \frac{\sigma_i^m}{\sigma_L^c} \tag{7}$$

`

where, the subscript L denotes the load case, i denotes the six components of the stress vector, f denotes the fiber, m denotes the matrix and c denotes the composite. For example the mapping functions for matrix constituent under a pure σ_{11} composite load state are

$$_1X_i^m = \frac{\sigma_i^m}{\sigma_1^c} \tag{8}$$

Thus for any composite load state, the stress i in a constituent a is given by

$$\sigma_i^a = \sum_{L=1}^{6} {}_L X_i^a \sigma_j^c \tag{9}$$

Results

The focus of this work is to use the Fertig failure theory to predict failure of composites and benchmark it against lamina failure test data [20][21] from well know composite failure benchmarks 'World Wide Failure Exercise-I' (WWFE-I) and 'World Wide Failure Exercise-II' (WWFE-II). The failure exercises contain in total twenty-six carefully selected test cases which include strength envelopes and stress-strain curves for a range of unidirectional and multidirectional laminates. This failure theory is benchmarked against seven strength envelopes for unidirectional laminae. These are ideal for evaluating failure criteria, whereas laminate level tests are appropriate for evaluating the combination of failure criteria with progressive damage methodology. The details of the test cases are included in Table 1. The results obtained were compared with leading theories from WWFE-I and WWFE-II discussed above.

Table 1

Test case	Lamina layup	Material	Loading
1	0°	E-glass/LY556 epoxy	σ_2 vs. τ_{12}
2	0°	T300/BSL914C carbon/epoxy	σ_1 vs. τ_{12}
3	0°	E-glass/MY750 epoxy	σ_2 vs. σ_1
4	0°	T300/PR319	τ_{12} vs. σ_2 ($\sigma_1 = \sigma_2 = \sigma_3$)
5	90°	E-glass/MY750 epoxy	σ_2 vs. σ_3 ($\sigma_1 = \sigma_3$)
6	0°	S-glass/epoxy	σ_1 vs. σ_3 ($\sigma_2 = \sigma_3$)
7	0°	Carbon/epoxy	σ_1 vs. σ_3 ($\sigma_2 = \sigma_3$)

The benchmarking of the theory and its comparison with the leading failure theories is shown below.

Test case 1: GRP lamina under combined transverse normal and shear loading
The failure envelopes predicted by the Fertig failure theory for case 1 are shown in Fig. 2. Figure 2(a) shows the failure envelope when the UD values provided by the WWFE-I authors were used as model inputs. Figure 2(b) shows the failure envelope obtained when different UD values were

`

used as inputs to the model which yielded slightly better results. In both the cases (a) and (b), the theory fits the shape of the test data very well especially in the $(+\sigma_2, \tau_{12})$ quadrant. In case (a), Fertig failure theory is conservative, especially in the $(-\sigma_2, \tau_{12})$ quadrant. By choosing a different transverse compressive strength than the one given by the originators of the exercise, the theory predicts a failure envelope which is a little less conservative.

(a)   **(b)**
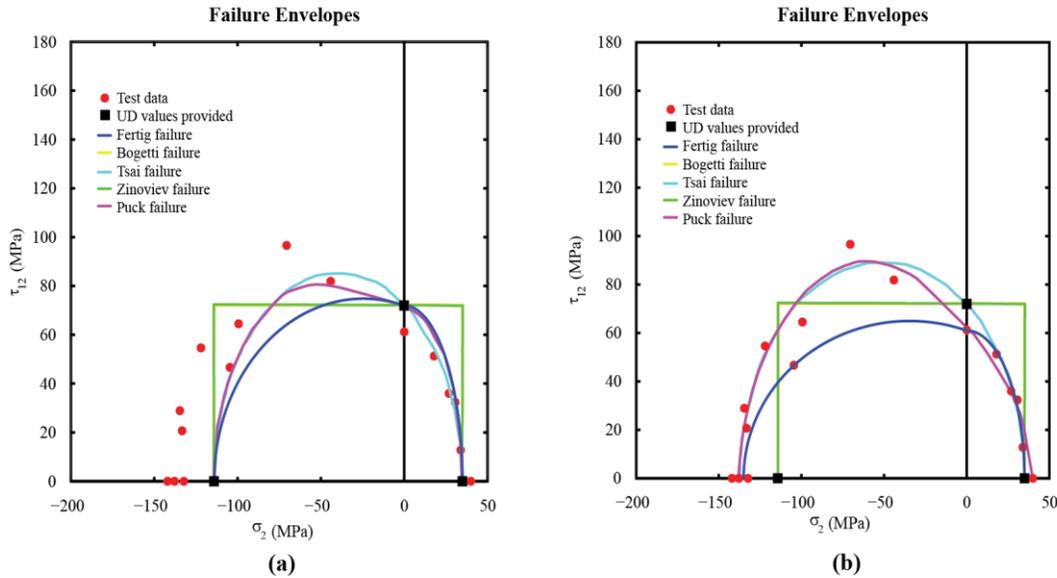
Figure 2. (a) Biaxial failure envelopes for 0° lamina made of GRP material (E-glass/LY556) with UD values provided as model inputs
(b) Biaxial failure envelopes for 0° lamina made of GRP material (E-glass/LY556) with different UD values as model inputs

Test case 2: GRP lamina under combined longitudinal and shear loading

The failure envelopes predicted by the Fertig failure theory for test case 2 are shown in Fig. 3. It can be seen that the theory captures the general shape of the experiments very well except in the high-shear region. It is known that material inhomogeneity in a composite gives rise to stress and strain fluctuations in the constituents. We have already shown that the volume average matrix stresses do not capture these stress/strain fluctuations in the constituents of the composite material and thus all the strain energy of a constituent is not accounted for [22]. The bulk of this missing energy (about 30%) is due to fluctuations in the matrix constituent when the composite is a under shear state of stress. Because our failure theory uses volume average constituent level stresses to predict failure of the constituents of the composite material, the

Figure 3.Biaxial failure envelopes for 0° lamina made of CFRP material (T300/914C)

matrix failure in this high shear region is not captured well since the missing strain energy in the matrix constituent is ignored. The matrix failure theory needs to be augmented with this missing energy to improve the predictions for this test case.

`

Test case 3: CFRP lamina under combined normal and longitudinal loading
The failure predictions of our failure theory and a modified failure theory are shown in Fig. 4. Figure 4(a) shows the failure envelope obtained using the original Fertig failure theory. It can be seen that like most of leading theories, the Fertig failure theory is very conservative in the
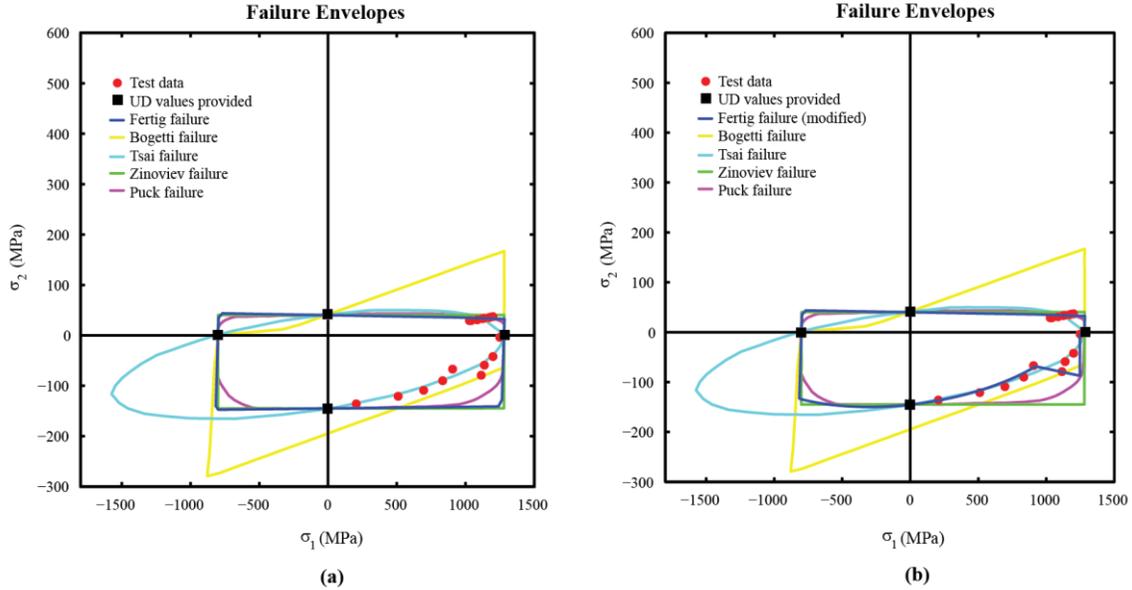
Figure 4. (a) Biaxial failure envelopes for 0° lamina made of GRP material (E-glass/MY750) with original Fertig failure
(b) Biaxial failure envelopes for 0° lamina made of GRP material (E-glass/MY750) with modified Fertig failure

$(+\sigma_1, -\sigma_2)$ quadrant.
Figure 4(b) shows the failure predictions of a modified Fertig failure theory which captures the shape of the experiments better than _any_ of the leading failure theories in WWFE-I.

This modified approach first requires the calculation of the matrix stress concentration factor in an ideal microstructure at the point of critical matrix failure under transverse tension. Figure 5 shows the fluctuations in the maximum principal matrix stress when the RVE with hexagonal fiber packing was subjected to transverse failure load.

S, Max. Principal
(Avg: 75%)
+5.117e+01
+4.656e+01
+4.195e+01
+3.734e+01
+3.273e+01
+2.812e+01
+2.351e+01
+1.890e+01
+1.430e+01
+9.686e+00
+5.077e+00
+4.672e−01
−4.142e+00
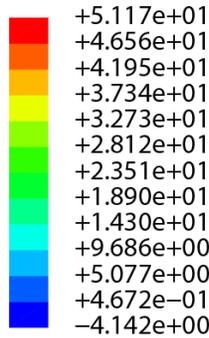
$\sigma_{Vavg} = 30.3866$ MPa
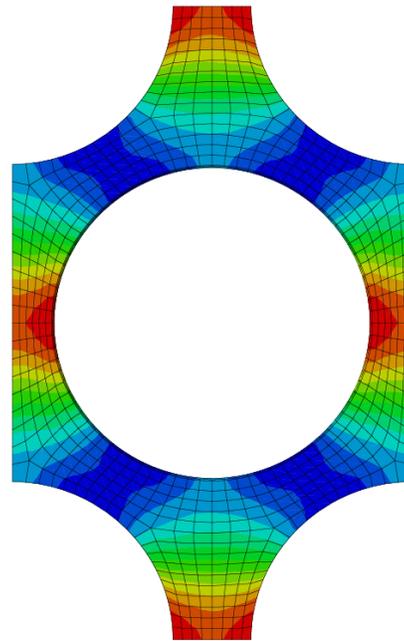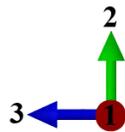
Figure 5: Fluctuations in maximum principal matrix stress

The matrix stress concentration factor (α_m) can be computed using the maximum and nominal (or volume average) stresses as follows

$$\alpha_m = \frac{\sigma_{\max}^m}{\sigma_{nom}^m} \tag{10}$$

where α_m is the matrix stress concentration factor

$\sigma_{\max}^m$ and σ_{nom}^m are maximum principal and nominal matrix stresses respectively

The modified matrix failure criteria is as follows

$$\frac{\sigma_{\max\ principal}^m}{S_{+t}^m \alpha_m} = 1 \qquad \text{or} \qquad \frac{\sigma_{VM}^m}{S_{VM}^m} = 1 \tag{11}$$

where $\sigma_{\max\ principal}^m$ is the maximum principal matrix stress

σ_{VMl}^m is the Von Mises stress in the matrix

S_{+t}^m is the transverse tensile strength of the matrix

S_{VM}^m is the Von Mises strength of the matrix

and α_m is the matrix stress concentration factor

The fiber failure criterion remains unchanged. In test case 3, it was observed that after the point of critical failure, the matrix failure was due to large principal stresses in the fiber direction. After this point even though the matrix was failing, the fiber could hold the composite together but it now it was carrying a larger load. To calculate the resultant fiber stresses after matrix failure, the matrix properties were degraded as follows

$$E_{new}^m = 15\% E_{original}^m \tag{12}$$

$$\upsilon_{new}^m = 0.01\% \upsilon_{original}^m \tag{13}$$

where E_{new}^m and $E_{original}^m$ are the new and original Elastic moduli of the matrix respectively and

υ_{new}^m and $\upsilon_{original}^m$ are the new and original poisons ratio of the matrix respectively.

The new resultant fiber stresses were computed from the RVE with hexagonal fiber packing using the procedure discussed in the second section (Failure Modeling). The original fiber failure criterion and new fiber stresses were then used to compute failure load which represents catastrophic composite failure. The modified approach was used to predict failure load in the ($-\sigma_1, -\sigma_2$) and ($+\sigma_1, -\sigma_2$) quadrants while the original Fertig failure theory was used in the remaining two quadrants.

Test case 4: Combined hydrostatic and shear loading
The failure envelopes predicted by the Fertig failure theory for test case 4 are shown in Fig. 6. Figure 6(a) shows the failure envelope when the UD values provided by the authors were used as model inputs and β = 0.1 and Fig. 6(b) shows the failure envelope when different UD values were

`

used as inputs to the model and $\beta = 0.35$. In both the cases (a) and (b), the theory fits the shape of the test data very well. When the shear strength of the 0° tubes is used as one of the model inputs, the theory captures the test data of the 0° very well. When the UD values provided by the originators of the exercise are used, the pressure strengthening term β has to be reduced to 0.1 from 0.35 to capture the failure of 90° tubes.
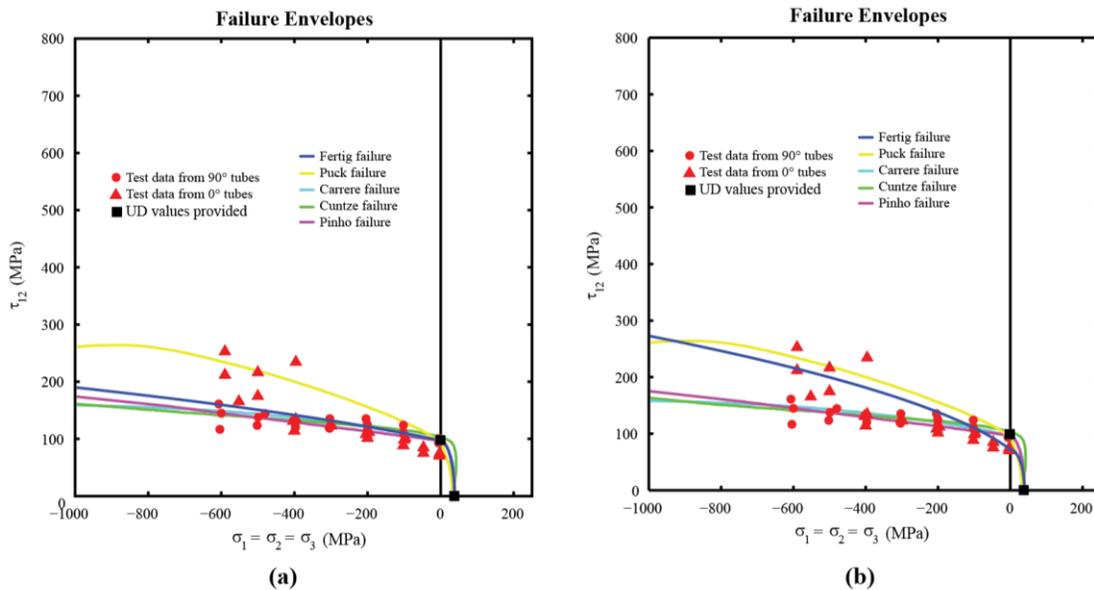
Figure 6. (a) Triaxial failure envelopes for 0° lamina made of CFRP material (T300/PR319) with UD values provided as model inputs and $\beta=0.1$
(b) Triaxial failure envelopes for 0° lamina made of CFRP material (T300/PR319) with different UD values as model inputs and $\beta=0.35$

Test case 5-7:
The failure envelopes predicted by the Fertig failure theory for test cases 5-7, which are omitted for space, are very similar to the other theories that have been compared. The exception is when the primary mode of failure is fiber kinking, where only two theories have been shown to be accurate, but require extensive calibration.

Conclusions

The failure envelopes from the Fertig failure theory were compared with the lamina failure test data from WWFE-I and WWFE-II. It was concluded for most of the test cases, the predictions of the theory were in close agreement with the test data. The predictions of the theory were also similar to the leading failure theories from the WWFE exercises. However, the leading theories from WWFE-I and WWFE-II require substantially more input parameters, which makes calibration very difficult. The merit of Fertig failure theory lies in its simplistic calibration, which requires just three parameters that can be obtained from three standard composite failure tests (transverse tension, transverse compression and in-plane shear). The modified Fertig failure theory, which is a two parameter theory, performed better than any of the leading failure theories in predicting the strength of the composite under combined transverse and longitudinal loads (Test case 3). Under combined longitudinal and shear loading (Test case 2), the Fertig failure theory did not predict the failure loads when the composite was under high-shear and low-longitudinal stresses. It has already been shown that the volume average matrix stresses do not

`

capture the stress/strain fluctuations in the constituents of the composite material and thus all the strain energy of a constituent is not accounted for especially under shear loading. Moreover, for commonly used fiber volume fractions, almost all of the strain energy is due to the fluctuations in the matrix constituent. Consequently, only the matrix failure needs to be augmented with this missing energy to improve on the predictions for the particular test case.

[1]   Jones, Robert M, vol. 2. London: Taylor & Francis, 1975.
[2]   Gibson, Ronald F, *Principles of composite material mechanics*, vol. Vol. 218. CRC press, 2012.
[3]   I. Daniel, "Failure of composite materials," *Strain*, vol. 43, no. 1, pp. 4–12, 2007.
[4]   S. W. Tsai and E. M. Wu, "A general theory of strength for anisotropic materials," *Journal of composite materials*, vol. 5, no. 1, pp. 58–80, 1971.
[5]   Z. Hashin and A. Rotem, "A fatigue failure criterion for fiber reinforced materials," *Journal of composite materials*, vol. 7, no. 4, pp. 448–464, 1973.
[6]   R. Christensen, "Stress based yield/failure criteria for fiber composites," *International journal of solids and structures*, vol. 34, no. 5, pp. 529–543, 1997.
[7]   A. Puck and H. Schürmann, "Failure analysis of FRP laminates by means of physically based phenomenological models," *Composites Science and Technology*, vol. 58, no. 7, pp. 1045–1067, 1998.
[8]   P. A. Zinoviev, S. V. Grigoriev, O. V. Lebedeva, and L. P. Tairova, "The strength of multilayered composites under a plane-stress state," *Composites science and technology*, vol. 58, no. 7, pp. 1209–1223, 1998.
[9]   K.-S. Liu and S. W. Tsai, "A progressive quadratic failure criterion for a laminate," *Composites Science and Technology*, vol. 58, no. 7, pp. 1023–1032, 1998.
[10]   T. A. Bogetti, C. P. Hoppel, V. M. Harik, J. F. Newill, and B. P. Burns, "Predicting the nonlinear response and progressive failure of composite laminates," *Composites science and technology*, vol. 64, no. 3, pp. 329–342, 2004.
[11]   M. J. Hinton, A. S. Kaddour, and P. D. Soden, "A comparison of the predictive capabilities of current failure theories   for composite laminates, judged against experimental evidence," *Compos. Sci. Technol.*, vol. 62, no. 12–13, pp. 1725–1797, 2002.
[12]   N. Carrere, F. Laurin, and J. Maire, "Micromechanical-based hybrid mesoscopic 3D approach for non-linear progressive failure analysis of composite structures," *Journal of Composite Materials*, vol. 46, no. 19–20, pp. 2389–2415, 2012.
[13]   S. Pinho, R. Darvizeh, P. Robinson, C. Schuecker, and P. Camanho, "Material and structural response of polymer-matrix fibre-reinforced composites," *Journal of Composite Materials*, vol. 46, no. 19–20, pp. 2313–2341, 2012.
[14]   R. Cuntze and A. Freund, "The predictive capability of failure mode concept-based strength criteria for multidirectional laminates," *Composites Science and Technology*, vol. 64, no. 3, pp. 343–377, 2004.
[15]   H. M. Deuschle and A. Puck, "Application of the Puck failure theory for fibre-reinforced composites under three-dimensional stress: Comparison with experimental results," *Journal of Composite Materials*, vol. 47, no. 6–7, pp. 827–846, 2013.
[16]   A. Kaddour and M. Hinton, "Maturity of 3D failure criteria for fibre-reinforced composites: Comparison between theories and experiments: Part B of WWFE-II," *Journal of Composite Materials*, vol. 47, no. 6–7, pp. 925–966, 2013.

`

[17]   Ray S. Fertig, III, "Bridging the gap between physics and large-scale structural analysis: a novel method for fatigue life prediction of composites.". [Accessed: 04-Sep-2012].

[18]   C. P. Hoppel, T. A. Bogetti, and J. W. Gillespie, "Literature Review-Effects of hydrostatic pressure on the mechanical behavior of composite materials," *Journal of Thermoplastic Composite Materials*, vol. 8, no. 4, pp. 375–409, 1995.

[19]   Ray S. Fertig, III, "A Computationally Efficient Method For Multiscale Modeling Of Composite Materials: Extending Multicontinuum Theory To Complex 3d Composites."

[20]   P. D. Soden, M. J. Hinton, and A. S. Kaddour, "Biaxial test results for strength and deformation of a range of E-glass and carbon fibre reinforced composite laminates: failure exercise benchmark data," *Composites Science and Technology*, vol. 62, no. 12–13, pp. 1489–1514, Sep. 2002.

[21]   M. J. Hinton and A. S. Kaddour, "Triaxial test results for fibre-reinforced composites: The Second World-Wide Failure Exercise benchmark data," *Journal of Composite Materials*, Sep. 2012.

[22]   Kedar A. Malusare and Ray S. Fertig III, "On the Use of Volume Average Constituent Stresses for Predicting Failure in Composites," presented at the 54th AIAA/ASME/ASCE/AHS/ASC Structures, Structural Dynamics, and Materials Conference, Boston, Massachusetts, 2013.

`